

Development of a Novel Intelligent Robotic Manipulator

George J. Vachtsevanos, Kent Davey, and Kok-Meng Lee

ABSTRACT: This paper describes the design features of a new robotic manipulator incorporating a novel spherical motor capable of three degrees of motion in a single joint for purposes of dexterous actuation, a loadable device at the end of the wrist actuator as the end effector with tactile and proximity sensing capabilities, and appropriate conventional and intelligent planning and control algorithms to support the execution of a series of complex tasks in an uncertain or hostile environment. The spherical wrist actuator is developed through analytic studies and the design of position and torque control instrumentation. The end effector is a micromanipulator based on the principle of in-parallel mechanisms. Heuristics, manifested in fuzzy logic, are employed to incorporate artificial intelligence for decision making and control in the robotic manipulator. The intent is to provide an overview of the significant design and algorithmic features of the manipulator deferring a detailed treatment of the proposed approaches to forthcoming publications.

Introduction

The performance of a robotic manipulator is usually defined in the context of the work task it is designed to perform. Speed, accuracy, dexterity, weight, complexity, and reliability are some of the performance measure attributes for robotic manipulators. Two fundamental issues that significantly influence the design of manipulators are structural rigidity and the interaction of the end effector with the workpiece or its environment in the process of performing tasks.

A number of researchers have addressed the design of fine-positioning devices with end-point sensing to enhance the robot accuracy [1]–[3] for purposes of electronic manufacturing. A design of a “Jig Hand” was suggested in [4] to bear the vibratory

interaction force during the machining operation. Bracing strategies have been proposed [5], [6], aiming to rigidize the base of the “wrist” for subsequent fine motion. In general, these approaches are primarily directed toward extending the overall robot performance in several dimensions by separating the manipulation into *coarse* motion of a general robot arm, particularly a flexible arm, and *fine* motion of a dexterous end effector.

Precision manipulation tasks often require small, high-bandwidth motions. The high bandwidth and accuracy needed for fine motions are principal reasons dexterous actuators with small weight-to-force ratios and innovative end effectors are sought in many designs.

Moreover, many robotic systems, such as a fine-motion micromanipulator, associated with complex automation tasks, are large-scale systems that defy accurate mathematical description or application of current control-theoretic techniques. This predicament has led many investigators to a consideration of heuristic-based methods for scheduling, planning, coordination, and control of such systems [7]. An intelligent controller for a complex large-scale system, such as a robotic manipulator, employs sensory perception to detect changes in its working environment, and, by its own decision-making faculty, proceeds with the proper planning and control operations. Autonomy, as manifested by intelligent control strategies, will be a necessary complement to dexterity if future robot manipulators are to meet the challenge of automation.

This work addresses the problems of autonomy via intelligent control. The latter requires, in addition to the AI (artificial intelligence)-based algorithmic developments, proper design and integration of component-level processes, including sensors, end-effector mechanisms, and actuators with adaptive and control-theoretic methods.

Figure 1 is an artist's rendering of the proposed manipulator basic components. They are discussed briefly in the following paragraphs. Basic design objectives include dexterity of locomotion, ability to resolve unforeseen or adverse situations, and fine task execution via intelligent planning and robot control.

Spherical Motor

Recent advances in robotics, intelligent end effectors, and flexible manufacturing systems have provided the motivation for the resurfacing of unusual designs with certain motors and electromechanical transducers. A flurry of research activity is currently under way in direct drives involving DC stepping and brushless electromechanical actuators. These devices are normally employed to accomplish a single degree of motion manipulation at each joint. The spherical induction motor presents attractive possibilities for combining pitch, roll, and yaw motion in a single joint, while maintaining the control functions required for completing its manipulation tasks. Williams et al. [8], [9] and Laithwaite [10] performed the original analysis on one form of spherical induction motor. General flux linkage arguments and es-

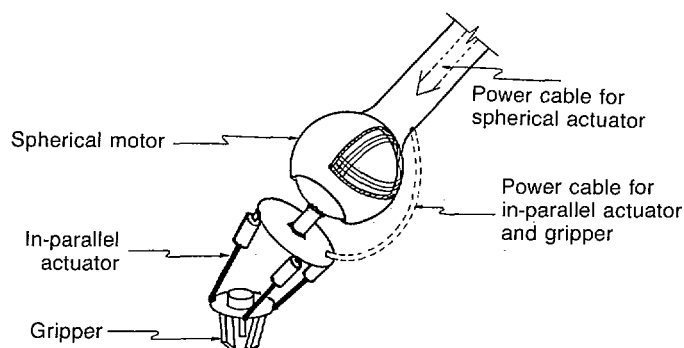


Fig. 1. Proposed micromanipulator.

Presented at the 1986 IEEE International Conference on Systems, Man, and Cybernetics, Atlanta, Georgia, October 14–17, 1986. George J. Vachtsevanos and Kent Davey are with the School of Electrical Engineering and Kok-Meng Lee is with the School of Mechanical Engineering, Georgia Institute of Technology, Atlanta, GA 30332.

imates of magnetic diffusion times were used to predict forces and torques on a realization of the device that was built and successfully tested. Here, the application was in speed control—achieved by controlling the direction of the stator wave excitation at an arbitrary angle to the motor axis. Since the work in [8]–[10], little attention has been given to the spherical motor, with the exception of a patent, some gyroscope applications, and a Russian paper [11] containing a theoretical analysis.

A pictorial representation of the proposed motor is shown in Fig. 2. Three sets of windings are necessary to realize rotation about an arbitrary axis. The three windings are positioned to give rotations about the x , y , and z axes when each is independently excited. By independently controlling the strength and phase of any two windings, one can realize a rotation vector at any point in the rotation plane of these two windings. A second realization of the spherical actuator is based upon a stepper motor principle. The stepper design is simpler to implement, since it does not entail such physical constraints as placing three transverse three-phase windings into the inner spherical stator shell. In this arrangement, the stator consists of a number of iron teeth, each with an isolated spool-type excitation winding. The rotor consists of one or more permanent magnets having the same cross-sectional area as the stator teeth. The individual teeth must be energized sequentially to pull the rotor to any

position desired. With two rotor magnets, more torque can be realized, but now a pair of teeth must be energized to coordinate force superposition. By slightly offsetting the rotor magnets so as not to be exactly aligned with the teeth spacing, a finer degree of control movement can be realized. A stepper spherical motor prototype is currently under construction.

A general analysis of both the fields and resultant forces generic to the spherical induction motor has been completed. The analysis properly accounts for the diffusion of the magnetic field with changing frequency and motor speed. The first analysis step involves a general representation of the fields in the conductor constituting the secondary member due to one stator winding. The effect of three windings is arrived at using superposition.

The philosophy in this development follows:

- (1) Isolate the excitation of the stator windings into two transverse components.
- (2) For each transverse component, solve the vector Helmholtz equation for magnetic fields in the air gap commensurate with the stator excitation.
- (3) Use the Maxwell stress tensor integrated over the annulus of the motor to predict the time-average torques in mutually transverse directions.
- (4) Integrate the flux density so derived over the surface area of the stator winding to

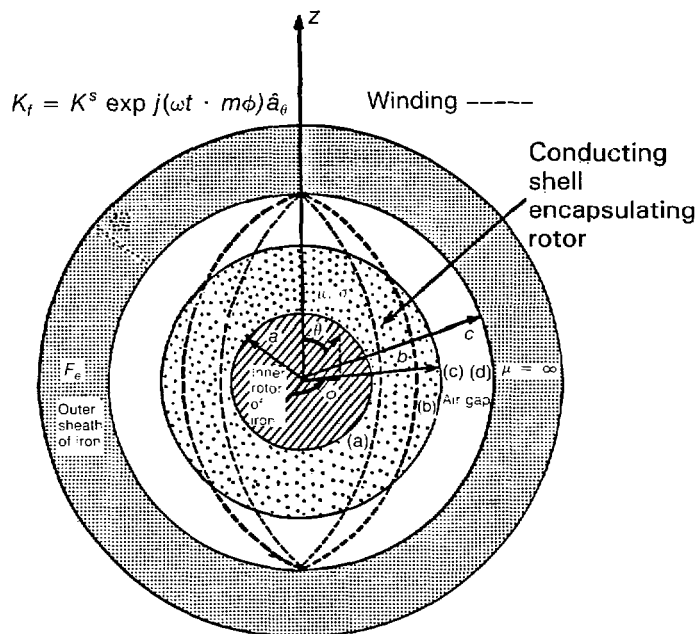


Fig. 2. Cross section of spherical induction motor. Rotor consists of conducting ball of thickness $(b-a)$ filled with infinite μ material.

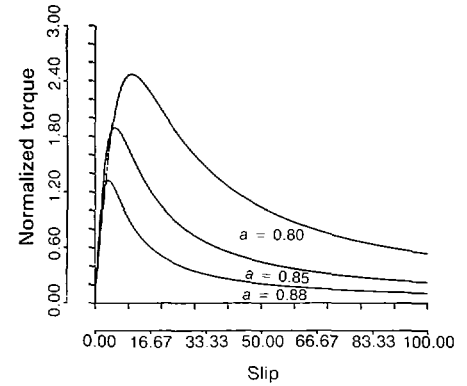


Fig. 3. Normalized torque vs. slip, $\alpha\sigma b^2(\omega - m\Omega)$, for spherical motor as rotor radius is varied.

determine the flux linkage and, thus, the terminal relations. The component of current in phase with the stator voltage represents stator/rotor resistive current and torque-generating current.

The nature of the fields necessitates an analytical representation in terms of Legendre polynomials. The details of the calculations are shown in a forthcoming paper [12]. Expressions for torque and flux linkage are derived. Typical results for torque vs. slip as the rotor radius is varied are shown in Fig. 3. Similarly, the flux linkage is shown in Fig. 4 as a function of slip; that part of the inductance less the total value at zero slip is seen to be a sensitive indicator of speed. Finally, an important indicator of the spherical actuator performance is its ability to convert efficiently electrical power into mechanical power. Figure 5 shows the normalized rotor power dissipation vs. slip as the rotor radius is varied.

Control of the Spherical Actuator

In the design of the actuator itself and its control mechanisms, efficiency of operation,

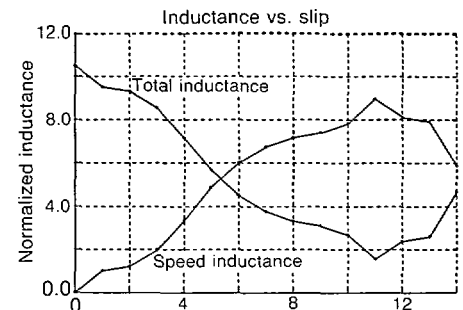


Fig. 4. Inductance vs. slip; total inductance (upper curve at slip zero) and speed inductance (lower curve).

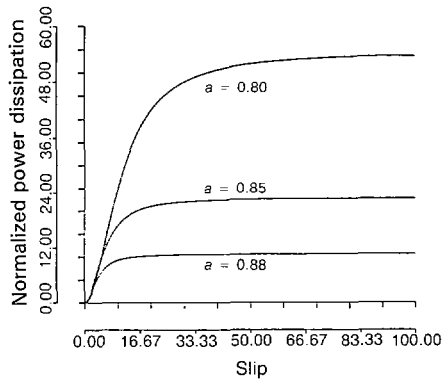


Fig. 5. Normalized rotor power dissipation vs. slip for spherical induction motor.

reliability of performance, and robustness are characteristics of primary concern. Induction motor drives have always been among the more robust electromechanical transducers, principally because of their simplicity of construction. The designer commonly finds a difficult trade-off between the choice of robustness imbedded in the induction motor versus the more simplistic control of direct current drives.

A modified hybrid position/force control philosophy has been adopted for the control of the spherical actuator. The basic hybrid position/force control architecture developed by Raibert and Craig [13] combines force and torque information with positional data to satisfy simultaneous position and force trajectory constraints specified in a task-related coordinate system. Their approach consists of separate position and force control loops. For a given task, the desired manipulator trajectories are specified in a task constraint frame, and natural position and force constraints are specified implicit to the task. A manipulation task can be broken down into elemental components that are defined by a particular set of contacting surfaces. A set of constraints, called the *natural constraints*, is associated with each elemental component. They result from the particular mechanical and geometric characteristics of the task configuration. A pin insertion problem is discussed in the sequel in conjunction with the development of appropriate task-oriented intelligent strategies. For each task configuration, a generalized surface is defined in a constraint space having N degrees of freedom. Natural position constraints are defined along the normals of the generalized surface, while natural force constraints are along the tangents to the surface. Additional artificial constraints are determined by the user when desired manipulator position and force trajectories are specified.

The constraint coordinate system $[C]$ is an N -degree-of-freedom Cartesian system defined with respect to the task geometry. Once the constraints for a given task are specified, they are used to partition the degrees of freedom into a position-controlled subset and a force-controlled subset. Furthermore, the desired position and force trajectories are prescribed through artificial constraints. Finally, the actuator control signal for the i th rotational axis has N components, one for each force-controlled degree of freedom in $[C]$ and one for each position-controlled degree of freedom:

$$\tau_i = \sum_{j=1}^N \{ \Gamma_{ij} [s_j \Delta f_j] + \Psi_{ij} [(1 - s_j) \Delta x_j] \}, \quad i = 1, 2, 3 \quad (1)$$

where N is the degrees of motion freedom in the C frame, τ_i the torque applied by the i th actuator winding, Δf_j the i th force error in the C frame, Δx_j the i th position error in the C frame, Γ_{ij} the force compensation function, Ψ_{ij} the position compensation function, and s_j the j th component of compliance selection vector s . If $s_j = 1$, then the j th primitive motion in the C frame is force-constrained. If $s_j = 0$, then the j th primitive motion in the C frame is position-constrained.

Torque sensing is accomplished via the force and position sensors situated on the longitudinal links of the in-parallel mechanism. The position feedback is achieved by implanting a small battery-driven oscillator circuit (1 kHz) on the rotor. The amplitude of a 1-kHz signal induced on the stator teeth infers position of the rotor at any time. Figure 6 illustrates the hybrid control system. Sensory signals are transformed from the coordinate system of the transducers into $[C]$ before the error signals are generated. A classical proportional, integral, derivative (PID) controller is used in each of the force and position loops. The net actuator signal is used to drive the stator input voltage. In parallel with the voltage control circuitry is a separate controller that sets the stator frequency. During an initial transient, the stator frequency on the windings is set, so as to yield maximum torque in the direction of the desired position/speed change for a given current on the winding. When the motor reaches the desired speed for a given action, the stator frequency is changed via an integral controller so as to minimize the losses in the system. The parallel combination of these control scenarios yields a motor controller, which is effective in realizing the desired torque, speed, and position objectives, as well as minimizing losses in the system;

it does so in a most efficient manner, so as to utilize expeditiously the current in the windings at any instant by maximizing torque generation. The basic principles were tested via simulation studies. The single winding dynamic operation of the motor is described by a set of four first-order differential equations in terms of the real and imaginary components of the rotor and stator currents, the applied stator voltage, and the motor equivalent circuit parameters representing winding self- and mutual-inductance and resistance. The dynamic rotor equation involving rotor inertia, drag, and load torque completes the dynamic description [14]. A Runge-Kutta differential equation solver is used to simulate the system's dynamic evolution. The control strategies are implemented between time steps, i.e., change in stator voltage or stator frequency. Several sensitivity runs indicate the effectiveness of the proposed control strategies.

End Effector

With a general-purpose robotic manipulator used as a coarse positioning device, a high torque-to-weight fine-motion robotic hand provides the dexterity and sensing capability. A closed kinematic chain actuated mechanism (as part of the micromanipulation end effector), with its associated sensors and high torque-to-weight actuator, is currently being investigated as an intelligent, fine-motion, high-precision robotic end effector.

The closed kinematic chain mechanism has been chosen for investigation. It has the following advantages as compared to the open kinematic chain mechanisms, which generally have the links actuated in series: higher torque/force for a number of actuators, better accuracy due to the lack of a cantileverlike configuration, and relatively simple inverse kinematics, which is important for real-time manipulator control. The concept of an in-parallel mechanism has been applied to a number of applications. Typical examples are a camera tripod and a six-degree-of-freedom steward platform, which was originally designed as an aircraft simulator. Recently, work has been directed toward tendon actuated in-parallel manipulators, which have the advantage of high force-to-weight ratio. The manipulation design analyzed is a three-degree-of-freedom in-parallel actuated manipulator, which has two degrees of freedom in orientation and one degree of freedom in Cartesian position.

A schematic of an in-parallel manipulator is shown in Fig. 7, with the base coordinate frame indicated as XYZ and the second co-

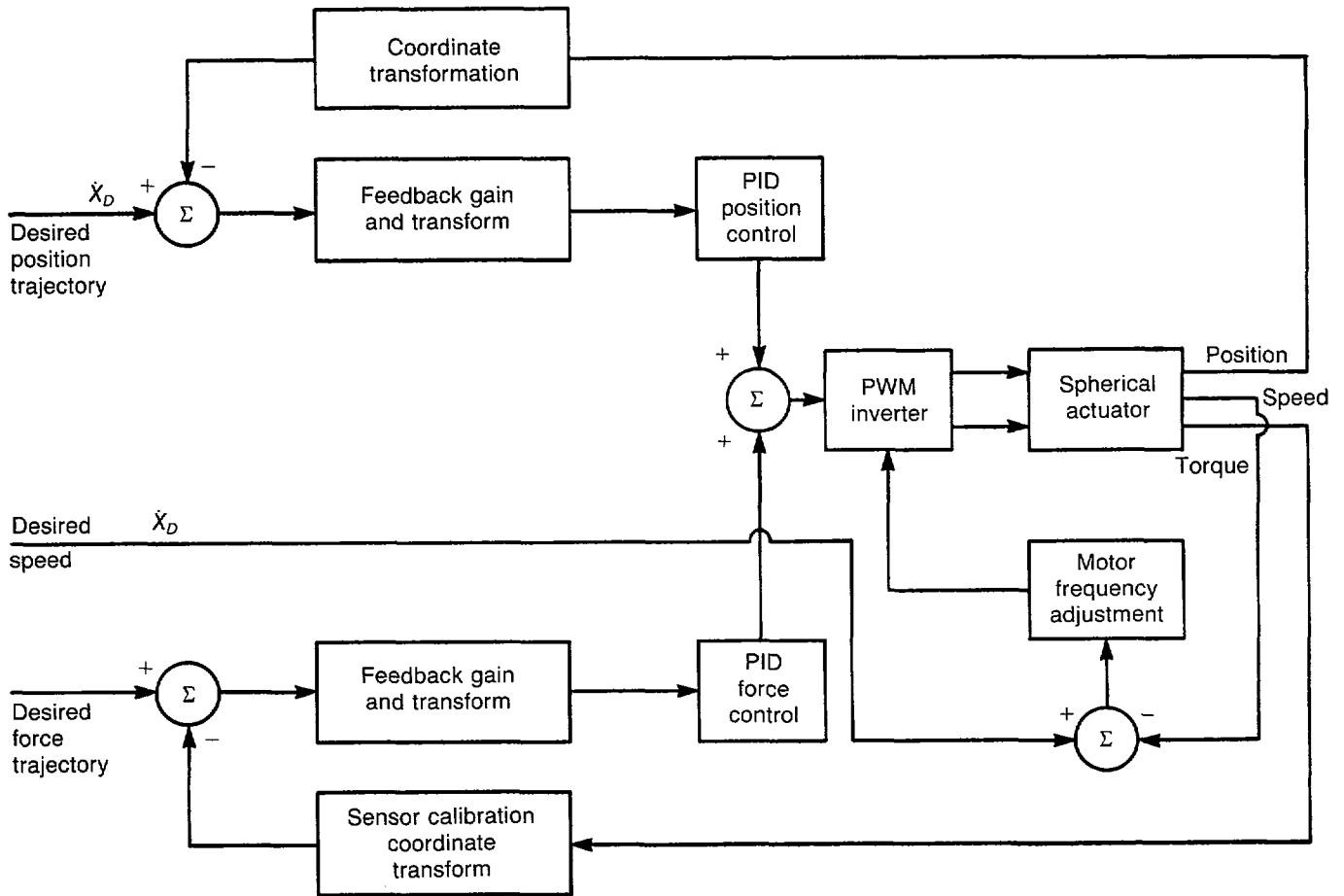


Fig. 6. Hybrid position/force control scheme for the spherical actuator.

ordinate frame xyz fixed at the moving platform shown in Fig. 8.

The coordinates of the pin and ball joints are specified first, and the position of the ball joints, with respect to the XYZ frame, is computed next. The inverse kinematic equations, which define the actuating lengths of the links for a specified position and orientation of the upper platform, are then derived in terms of six independent position/orientation variables. As the links are constrained by the pin joints to move in the planes $y =$

0 , $y = -\sqrt{3}x$, and $y = \sqrt{3}x$, respectively, there are three constraint equations imposed by the pin joints on the motion.

A closed-form solution for the lengths of the links for a predetermined trajectory has been derived in [15] in terms of Z - Y - Z Euler angles. The constraint equations are summarized as

$$\gamma = -\alpha \quad (2)$$

$$X_c = -\frac{1}{2}\rho(1 - C_\beta)C_{2\alpha} \quad (3)$$

$$Y_c = \frac{1}{2}\rho(1 - C_\beta)S_{2\alpha} \quad (4)$$

where $X_c = x_c/R$, $Y_c = y_c/R$, $\rho = r/R$, $C_\beta = \cos \beta$, $S_{2\alpha} = \sin 2\alpha$, $C_{2\alpha} = \cos 2\alpha$. α , β , and γ are precession mutation and spin angles of the Euler angles, respectively; R and r are radius from the center of the base and moving platforms, respectively; and x_c , y_c , and z_c are Cartesian position coordinates of the center of the moving platform with respect to the XYZ frame. The link lengths are

$$L_1^2 = 1 + \rho^2 + X_c^2 + Y_c^2 + Z_c^2 - 2X_c + 2\rho(C_\alpha^2 C_\beta + S_\alpha^2)(X_c - 1) + \rho(C_\beta - 1)S_{2\alpha}Y_c - 2\rho S_\beta C_\alpha Z_c \quad (5)$$

$$L_2^2 = 1 + \rho^2 + X_c^2 + Y_c^2 + Z_c^2 + X_c - \sqrt{3}Y_c - \rho[C_\alpha^2 C_\beta + S_\alpha^2 - \sqrt{3}C_\alpha S_\alpha(C_\beta - 1)] \times [X_c + \frac{1}{2}] - \rho[S_\alpha C_\alpha(C_\beta - 1) - \sqrt{3}(S_\alpha^2 C_\beta + C_\alpha^2)] [Y_c - \sqrt{3}/2] + \rho S_\beta [C_\alpha - \sqrt{3}S_\alpha] Z_c \quad (6)$$

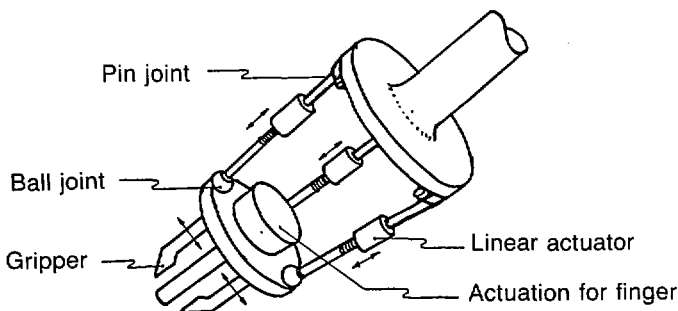


Fig. 7. In-parallel end effector.

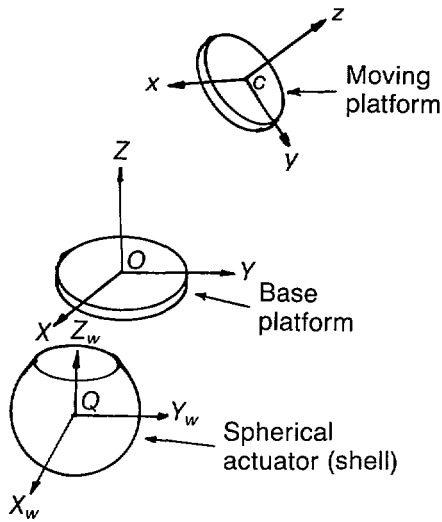


Fig. 8. Coordinate transformation.

$$\begin{aligned}
 L_3^2 = & 1 + \rho^2 + X_c^2 + Y_c^2 + Z_c^2 + X_c \\
 & + \sqrt{3}Y_c - \rho[C_\alpha^2 C_\beta + S_\alpha^2 \\
 & + \sqrt{3}C_\alpha S_\alpha(C_\beta - 1)] [X_c + \frac{1}{2}] \\
 & - \rho[S_\alpha C_\alpha(C_\beta - 1) \\
 & + \sqrt{3}(S_\alpha^2 C_\beta + C_\alpha^2)] [Y_c + \sqrt{3}/2] \\
 & + \rho S_\beta [C_\alpha + \sqrt{3}S_\alpha] Z_c \quad (7)
 \end{aligned}$$

where L_1 , L_2 , and L_3 are the link lengths normalized to R , $S_\alpha = \sin \alpha$, $C_\alpha = \cos \alpha$, $S_\beta = \sin \beta$, and $Z_c = z_c/R$. The constraint equations do not contain Z_c , and, hence, Z_c is essentially an independent variable. The other two independent variables may be the orientation variables α and β or the Cartesian position variables X_c and Y_c . For a prescribed position and orientation of the moving platform, the three dependent variables of the position/orientation must be computed from Eqs. (2)–(4), and the actuating lengths of the links are determined from the inverse kinematic equations (5)–(7).

Figure 1 shows a manipulator that combines an in-parallel actuated mechanism and a spherical wrist motor to form a six-degree-of-freedom manipulator system. As the spherical wrist motor has two positional degrees of freedom in addition to spin, the combined motion of the spherical motor and the in-parallel actuated mechanism results in a six-degree-of-freedom manipulating capability. The position/orientation of the gripper, with respect to the reference frame $X_w Y_w Z_w$ can be obtained using the homogeneous transformation $[T]$ as

$$[T] = [T_2] [T_1]$$

where $[T_1]$ is the coordinate transformation describing the coordinate frame xyz with respect to the base frame XYZ , and $[T_2]$ is the coordinate transformation that describes the position/orientation of the base frame XYZ with respect to the $X_w Y_w Z_w$ frame.

The equations of motion commensurate with an actuating force are derived for the in-parallel mechanism using a Lagrangian approach. Because the actuating forces acting along links F_1 , F_2 , and F_3 are to be found, the link lengths, l_i , and the angles between the links and base platform, θ_i , are chosen as generalized coordinates in which the link lengths l_1 , l_2 , and l_3 are independent. For a specified trajectory, the link length can be determined from the inverse kinematic equations. With the position of the i th ball joint expressed as a function of θ_i and l_i , the three equations that implicitly relate l_i and θ_i are obtained, noting that the distance between any two adjacent ball joints is constant.

An alternative approach to derive the inverse dynamics based on the independent generalized coordinates α , β , Z_c and the 3×3 Jacobian, which relates the actuating lengths to orientation and axial freedoms (α , β , Z_c), has been described in [15].

The uses of robotic manipulators are increasingly important in data-driven manufacturing, automated assembly, and intelligent machining. It is noted that both the precise end-point position/orientation control and the constrained motion control are important in the manipulator applications. The former involves control of the three actuating links, and the latter requires control of the corresponding actuating forces along the links.

The in-parallel actuated end effector is essentially a rigid structure for a given set of link lengths. Hence, one obvious scheme is to sense and control the three actuating lengths. Three additional sensors may be located to measure the angles between the links and base platform. Hence, the ball-joint positions can be determined directly from sensor information, and the Cartesian position of the moving platform can be determined by noting that the ball joints are essentially located at the vertices of an equilateral triangle. This sensing scheme avoids time-consuming numerical computation from the implicit relationships, which may be a drawback for real-time on-line microprocessor control.

The reaction forces and moments acting on the end-point can be sensed by measuring the forces along the links. Hence, in the control of the in-parallel actuated end effector, when the device is constrained by the task geometry, the actuating links are essentially

the sources of active compliance, where the actuating forces along the links are measured and fed back.

The manipulator dynamics are described by a set of highly nonlinear, coupled, time-varying, ordinary differential equations [15] for which closed-form analytical solutions may not be available. Instead, solutions to these equations can usually be obtained by numerical integration on a digital computer. Also, in manipulator applications, substantial uncertainty in the system characteristics is introduced by the unknown payload mass properties. Hence, the model reference adaptive control scheme is being investigated for the control of the in-parallel actuated manipulator.

The proposed controller design consists of a first-order fixed compensator in the inner loop and an adaptive controller in the outer loop. The purpose of the fixed compensator is to reduce the effect of the unmodeled coupling force/torque and, therefore, ease the effort of the adaptive controller. In the design of the adaptive controller for each actuating link, the coupling force acting on the link is neglected. However, the fixed compensator is kept in the inner loop as a part of the actual manipulator system.

For the development of the adaptive control algorithm, the dynamics of each link may be approximated as

$$\ell(s) = G(s) [F_i(s) + F(s)] \quad (8)$$

where ℓ is the length of the i th link to be controlled, F the actuating force along the link, F_i the force exerted by the moving platform on the link and is treated as plant uncertainties accountable for neglected nonlinear manipulator dynamics and the coupling of the system degrees of freedom, $G(s)$ the dynamics of the link and its actuating mechanism, and s a Laplacian operator.

The Intelligent Controller

The goals of assembly research over the past years have been to create machines that would show the flexibility and tolerance of errors in parts and fixtures and would also show the experience and speed of trained human operators. The part-mating problem has been attacked by analyzing, in a quasi-static setting, the geometry of idealized task situations and determining what moments, contact and friction forces will occur in response to specific relative part positions [16]. Proposed control strategies include passive compliance devices and several active compliance means that use move-and-bump experiments to enumerate cases of relative positions that could occur and pro-

programming a sequence of test moves to determine which case is in effect [17], [18]. Another approach strives to use force-torque data from the assembly action itself to direct the fine motions and to eliminate test motions where possible.

The approach pursued here is to design intelligent control algorithms that will permit the robotic manipulator to behave in a semi-autonomous manner by using a variety of sensor data, dexterous actuators, and flexible end effectors to perform complex tasks in an uncertain environment.

The intelligent controller of the manipulator must be capable of interfacing with local dynamic controllers (position, velocity, torque, etc.) so that task planning and coordination strategies generated by the intelligent controller are converted to command signals required to drive the conventional control modules.

An intelligent multivalued controller is being developed to assist in automating the performance of the manipulator in three basic tasks: obstacle avoidance, a jig and fixture assembly process, and a pin placement problem.

Consider the pin insertion problem depicted in Fig. 9. The robot arm has positioned the wrist/end effector workpiece assembly over the hole via gross motion. The actual insertion is accomplished next by utilizing the manipulative fine-motion capabilities of either the end effector alone, as shown in the figure, or the wrist/end effector combination. When the pin is located in the im-

mediate vicinity of the hole, vision and proximity sensing is usually obstructed and the mating task must rely on information obtained from force-torque sensors. Reaction forces and friction forces may be estimated by monitoring the longitudinal forces and link positions of the in-parallel mechanism. Computational efficiency is improved by casting the intelligent controller relationship into a production system. The latter consists of a knowledge base of production rules; a global data base, which represents the system status; and a rule interpreter (control structure) for choosing the rules to execute. A typical production rule for the situation depicted in Fig. 10 may be of the form: IF F_x is low and F_y is high and θ is small and D is low, THEN move the end effector up slightly and rotate it by a medium angle.

In order to incorporate uncertainty, the linguistic variables low, high, etc., are modeled as fuzzy membership functions. The rule interpreter receives current information from the global data base and fires those rules whose antecedent sides are matched by the sensor data. The control action is estimated from the active rule set by using the principle of modus ponens. The intelligent algorithm thus breaks up the control task into elemental components that provide the required set points of the local end effector or wrist control modules. The integration philosophy is depicted in block diagram form in Fig. 11.

The basic intelligent control algorithm may be implemented using a parallel microprocessor structure. Such rule-based algorithms

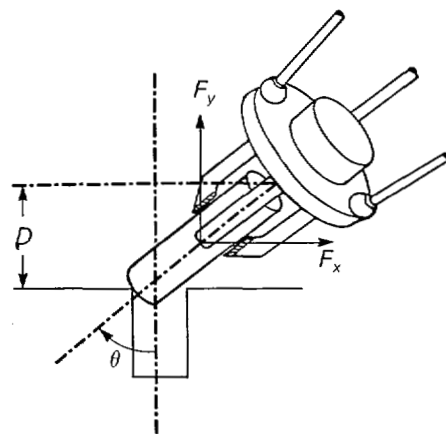


Fig. 10. Forces and positions for the pin insertion problem.

for MIMO (multi-input, multi-output) systems have the property of decomposing or decoupling the multivariable control input into a set of single-input, multi-output plants. It allows for a parallel controller structure using a common rule base that is easily implementable on an array of microprocessors.

Conclusions

A robotic manipulator is described incorporating a new spherical motor capable of three degrees of motion in a single joint for purposes of dexterous actuation, a loadable device at the end of the wrist actuator as the end effector, and appropriate conventional and intelligent planning and control algorithms to support the execution of a series of complex tasks in an uncertain or hostile environment. Further analytic studies and simulations are being conducted to ascertain the

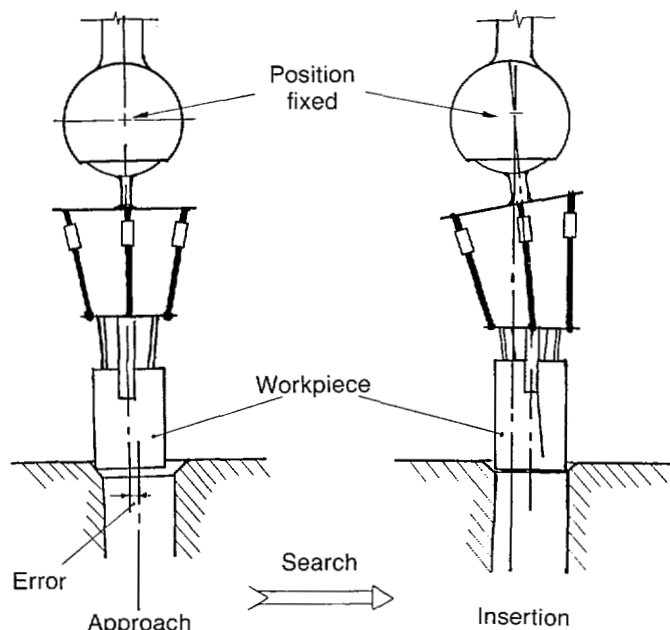


Fig. 9. Pin insertion using the micromanipulator.

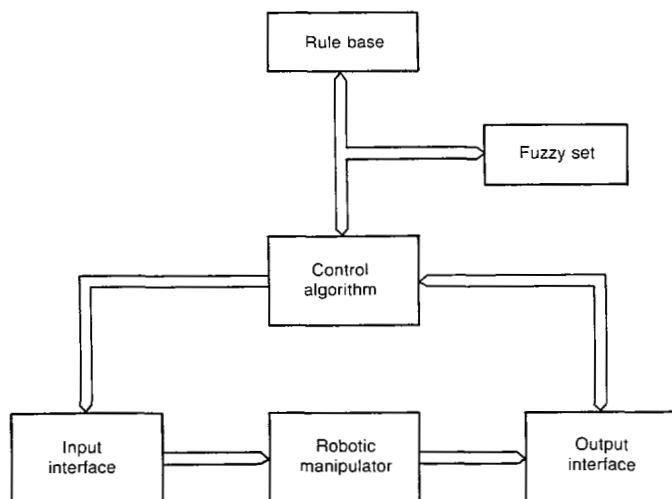


Fig. 11. Block diagram of the intelligent controller interface.

feasibility of the major manipulator components and the effectiveness of the proposed algorithmic approaches.

The spherical actuator provides for a robust device that can be exploited for both macro- and micromanipulation tasks. The in-parallel mechanism end effector enhances the flexibility and dexterity of the manipulator. The control strategies are designed to guarantee computational speed, robustness, and accuracy. A laboratory-scale prototype is currently being constructed to show proof of feasibility and to assist in refining and optimizing the manipulator design features.

References

- [1] R. H. Taylor, R. Hollis, and M. A. Lavin, "Precise Manipulation with End-Point Sensing," *IBM J. Res. Develop.*, vol. 29, no. 4, July 1985.
- [2] R. L. Hollis et al., "Robotic Circuit Board Testing Using Fine Positioners with Fiber-Optic Sensing," *Proc. Int. Conf. Industrial Robots*, Tokyo, Japan, Sept. 1985.
- [3] A. Sharon and D. Hardt, "Enhancement of Robot Accuracy Using End-Point Feedback and a Macro-Micro Manipulator System," *American Control Conf. Proc.*, San Diego, CA, pp. 1836-1842, June 6-8, 1984.
- [4] H. Asada and H. West, "Kinematic Analysis and Design of Tool Guide Mechanisms for Grinding Robots," 1984 ASME Winter Annual Meeting.
- [5] W. Book et al., "The Bracing Strategy for Robot Operation," Joint IFTOMM-CISM Symposium on the Theory of Robots and Manipulators (RoManSy), Udine, Italy, June 1984.
- [6] W. Book et al., "Combined Approaches to Lightweight Arm Utilization," *Robotics and Manufacturing Automation*, ASME vol. PED, vol. 15, pp. 97-108, Nov. 1985.
- [7] D. Nitzan, "Development of Intelligent Robots: Achievements and Issues," *IEEE J. Robotics and Automation*, vol. RA-1, pp. 3-13, Mar. 1985.
- [8] F. Williams, E. Laithwaite, and L. Piggot, "Brushless Variable-Speed Induction Motors," *Proc. IEEE*, no. 2097U, pp. 102-118, June 1956.
- [9] F. Williams, E. Laithwaite, and G. F. Eastham, "Development of Design of Spherical Induction Motors," *Proc. IEEE*, no. 3036U, pp. 471-484, Dec. 1959.
- [10] E. Laithwaite, "Design of Spherical Motors," *Electrical Times*, vol. 9, pp. 921-925, June 1960.

- [11] A. Rozouskii and L. Sunolobova, "Electromagnetic Processes in an Asynchronous Motor with a Spherical Hollow Rotor," *Bulletin of the Institutions of Higher Education Electromechanics* (Russian), vol. 11, pp. 1231-1239, Nov. 1976.
- [12] K. Davey, G. Vachtsevanos, and R. Powers, "The Analysis of Fields and Torques in a Spherical Induction Motor," *IEEE Trans. Magnetics*, Vol. MAG-23, No. 1, pp. 273-282, Jan. 1987.
- [13] M. H. Raibert and J. J. Craig, "Hybrid Position/Force Control of Manipulators," *Trans. ASME, J. Dyn. Syst., Measure., Contr.*, vol. 102, pp. 126-133, June 1981.
- [14] K. Davey and G. Vachtsevanos, "On the Control of a Novel Spherical Robotic Actuator," *Proc. 25th IEEE CDC*, Athens, Greece, Dec. 1986.
- [15] K.-M. Lee, A. Chao, and D. Shah, "A Three Degree of Freedom In-Parallel Actuated Manipulator," *Proc. IASTD 2nd Int. Conf. Applied Contr. and Identification*, Los Angeles, CA, Dec. 1986.
- [16] D. E. Whitney, "Quasi-Static Assembly of Compliantly Supported Rigid Parts," *J. Dyn. Syst., Measure., Contr.*, vol. 104, pp. 65-67, Mar. 1982.
- [17] J. L. Nevins and D. E. Whitney, "Research on Advanced Assembly Automation," *Computer*, pp. 24-38, Dec. 1977.
- [18] T. Goto, T. Inoyama, and K. Takeyasu, "Precise Inert Operation by Tactile Controlled Robot 'HI-T-HAND' Expert 2," *Proc. 4th Int. Symp. Industrial Robots*, pp. 209-218, Nov. 1974.



George J. Vachtsevanos was born in Kozani, Greece, in 1938. He received a B.E.E. degree from the City College of New York, an M.E.E. degree from New York University, and a Ph.D. degree in electrical engineering from the City University of New York (CUNY). Dr. Vachtsevanos was a member of the faculty of CUNY and Manhattan College before joining the faculty of the Democritus University of Thrace in Greece in 1978. In 1984, he became a Professor of Electrical Engineering at the Georgia Institute of Technology. His research interests include the development and control of electrical

actuators and the design of intelligent control strategies for hierarchical control and fault diagnostics. Dr. Vachtsevanos has published in the areas of controls, power systems, and instrumentation. He is a member of Eta Kappa Nu, Tau Beta Pi, and Sigma Xi.



Kent Davey was born in New Orleans, Louisiana, in 1952. He received the B.S. degree in electrical engineering in 1974 from Tulane University, New Orleans, Louisiana, the M.S. degrees in physics from the University of Pittsburgh and in power engineering from Carnegie-Mellon, both in 1976, and the Ph.D. degree in

electrical engineering from the Massachusetts Institute of Technology in 1980. During the years 1974-1976, he worked for Westinghouse Corporation as a Development Engineer analyzing fields and forces in large turbine generators. From 1979 to 1980, he worked at Texas A&M University as an Assistant Professor in electrical engineering. There he worked on magnetic induction devices suitable for energy storage purposes. From 1980 to present, he has worked at Georgia Tech, Atlanta, Georgia, where he is now an Associate Professor. His research interests include electric and magnetic field interaction with biological tissue, numerical solution of electromagnetic scattering problems, and prediction of fields in magneto-quasistatic problems, both transient and steady state.



Kok-Meng Lee was born in Singapore. He received the B.S. degree in mechanical engineering from the State University of New York at Buffalo in 1980 and the S.M.M.E. and Ph.D. degrees from the Massachusetts Institute of Technology, Cambridge, Massachusetts, in 1982 and 1985, respectively. Since 1985, he has

held an Assistant Professor appointment with The George W. Woodruff School of Mechanical Engineering, Georgia Institute of Technology, Atlanta, Georgia. His research interests are in the areas of system dynamics, design, and automatic control.